Chemical Geology 670 (2024) 122409

Contents lists available at ScienceDirect

Chemical Geology

journal homepage: www.elsevier.com/locate/chemgeo

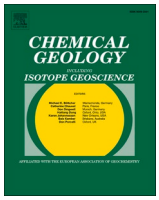

Terrestrial input and biological processes drive varying mineral/organic matrix-related mercury sequestration and deposition in the East Siberian Arctic Shelf

Jiazong Du [a], Limin Hu [a,b,*], Zhengquan Yao [b,c], Xiting Liu [a,b], Yifang Sun [a], Gang Yang [b,c], Kirill Aksentov [d], Yuriy Vasilenko [d], Alexander Bosin [d], Anatolii Astakhov [d], Xuefa Shi [b,c]

[a] College of Marine Geosciences, Key Laboratory of Submarine Geosciences and Prospecting Techniques, Ocean University of China, Qingdao 266100, China
[b] Laboratory for Marine Geology, Qingdao Marine Science and Technology Center, Qingdao 266237, China
[c] First Institute of Oceanography, Ministry of Natural Resources, Qingdao 266061, China
[d] V.I. Il'ichev Pacific Oceanological Institute, Far Eastern Branch Academy of Science, Russia

ARTICLE INFO

Editor: Dr. Hailiang Dong

Keywords:
Mercury
Organic carbon
Mineral matrix
Terrestrial input pathways
Primary productivity
East Siberian Arctic Shelf

ABSTRACT

Thawing Arctic permafrost is releasing massive amounts of terrestrial mercury (Hg) into the Arctic shelf, which is expected to form a Hg sink in sediments. Here we analyzed the coupling roles of terrestrial input and biological processes in varying mineral/organic matrix-related Hg sequestration and deposition on the East Siberian Arctic shelf (ESAS), using Pearson and partial correlation analysis. Results show that the occurrence of Hg in the Laptev Sea under the Lena River-dominated input exhibits strong correlations with the organic carbon (OC) content and sediment specific surface area. This indicates that the prolonged riverine loading processes facilitate Hg sequestration by organic/mineral matrices and these land-derived mineral-OC-Hg complexes remain stable during cross-shelf transportation. By contrast, the comparative samples with coastal erosion-dominated Hg input in the western East Siberian Sea shows limited Hg complexation, primarily due to the absence of regulation by riverine processes and/or the high sedimentation rates. The correlations between Hg and OC source proxies ($\delta^{13}C$ and lignin) indicate that these matrix-free Hg could be more readily sequestrated by the marine OC, which facilitates its deposition via the biological pump. While unexpectedly low Hg abundance in the Chukchi Sea may indicate that the effective biological scavenging of Hg sequestration could be constrained by insufficient terrestrial Hg input. Our findings of the matrix-related Hg sequestration by mineral and/or OC association in this study may shed light on the biogeochemical cycle of Hg in the Arctic aquatic regime, which could reduce the methylmercury formation in water column, and the methylation within sediments needs further exploration.

1. Introduction

Mercury (Hg) is a global concerning natural and anthropogenic pollutant. Despite the absence of local anthropogenic Hg emissions, the Arctic Ocean has become a hotspot for Hg accumulation due to the remobilization of Hg from permafrost (Durnford et al., 2010). The Arctic permafrost is a huge Hg pool with approximately 597 Gg stored in the upper 1–3 m (Lim et al., 2020). The ongoing global warming is gradually unlocking the Hg trapped within the permafrost (Rydberg et al., 2010; St Pierre et al., 2018), leading to its release and potential environmental impacts (Lim et al., 2019; Rydberg et al., 2010). Therefore, the climate-driven translocation of permafrost Hg to the Arctic shelf is expected to deliver more Hg to the Arctic Ocean and Arctic shelf sediments.

The biogeochemical processes of Hg in sediments affect its bioavailability in both the regional and global Hg cycles (Sun et al., 2023). The distribution and accumulation of Hg in sediments are controlled by the organic carbon (OC) and/or mineral matrices. OC has important effects on the total Hg (THg) concentration and activity in sediments by providing Hg binding sites (Park et al., 2018; Ravichandran, 2004). A significant positive correlation has been reported between total OC (TOC) and THg concentration in surface sediments from various estuarine, coastal, and open sea regions (Coquery et al., 1995;

* Corresponding author at: College of Marine Geosciences, Key Laboratory of Submarine Geosciences and Prospecting Techniques, Ocean University of China, Qingdao 266100, China.
E-mail address: hulimin@ouc.edu.cn (L. Hu).

https://doi.org/10.1016/j.chemgeo.2024.122409
Received 15 August 2024; Received in revised form 11 September 2024; Accepted 11 September 2024
Available online 13 September 2024

Hammerschmidt and Fitzgerald, 2004; Mason and Lawrence, 1999; Sanei et al., 2011; Stoichev et al., 2004). However, it has also been reported that THg concentration does not always increase with increasing TOC in sediments (Kehrig et al., 2003; Wu et al., 2013), primarily due to the varying affinity of OC for Hg depending on the OC sources and properties within different sedimentary systems. The marine OC shows stronger affinity for Hg than terrestrial OC due to the high chemical reactivity of these labile compounds (Sanei and Goodarzi, 2006; Stern et al., 2009). In addition, in sediments with limited OC content, higher THg concentration typically occurred in complexes with clay-silt particles, due to adsorption with large specific surface area (SSA) (Chakraborty et al., 2014). For example, clay minerals that are characterized by negatively charged surfaces and high cation exchange capacity show exceptional efficiency for the adsorption of heavy metals, including Hg (Brigatti et al., 2005; Phothitontimongkol et al., 2009). Therefore, the primary driving forces of sedimentary Hg vary with respect to different depositional environments and matrix-based affinity. Previous studies have focused on the Arctic Hg geochemistry and spatial distribution (Kim et al., 2023; Liem-Nguyen et al., 2022). Nevertheless, our understanding of the matrix-related constraints governing Hg distribution and accumulation within the Arctic shelf remains limited, highlighting the urgent need for further affinity mechanism research of Hg sequestration in this area.

The input of Hg from terrestrial permafrost through pan-Arctic rivers and coastal erosion is the largest net source of total Hg to the Arctic Ocean (Fisher et al., 2012). Rivers play a vital role in mobilizing and transporting the terrestrial Hg released from permafrost and up to 41 Mg yr^{-1} of Hg has been estimated to be delivered into the Arctic shelf via riverine input (Dastoor et al., 2022). In addition, coastal erosion can also release substantial quantities of permafrost OC and Hg into the shelf, with fluxes of 6.69 Tg yr^{-1} and 39 Mg yr^{-1}, respectively (Dastoor et al., 2022; Rachold et al., 2004). The translocation of sediments, terrestrial

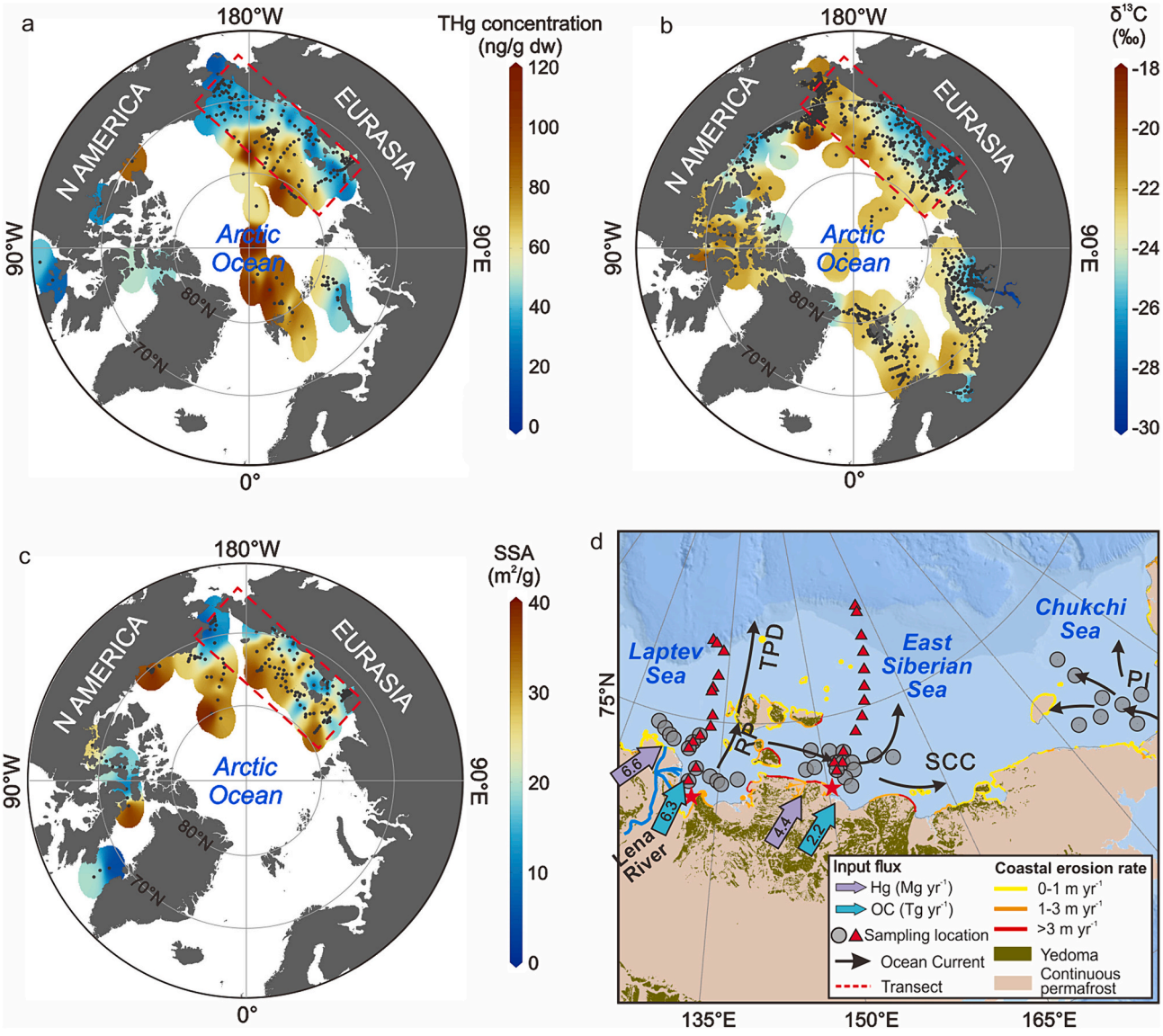

Fig. 1. The interpolated THg concentration (a), $\delta^{13}C$ values (b), and SSA (c) in the surface sediments of the pan-Arctic shelf seas (sampling sites in black dots). THg concentrations and SSA values were collected from published data (Tables S2 and S3) and $\delta^{13}C$ values were taken from CASCADE (Martens et al., 2021) (https://bolin.su.se/data/cascade). (d) Map of the study area in the ESAS. Grey circles and red triangles represent samples from the coastal regions and along the transects, respectively. The input fluxes of OC and Hg through the Lena River and coastal erosion are labeled in the LS and WESS, respectively. Red stars indicate the collection sites for mass accumulation rates (Martens et al., 2022; Vonk et al., 2012). The coastal erosion rates are indicated by yellow, orange, and red lines (Lantuit et al., 2012). Typical currents are shown by arrows following Tesi et al. (2016): RP, river plume; TPD, Transpolar Drift; SCC, Siberian coastal current; PI: Pacific inflow. (For interpretation of the references to colour in this figure legend, the reader is referred to the web version of this article.)

OC, and Hg via rivers undergoes long-term fluvial processes, whereas coastal erosion results in a rapid discharge and deposition of terrestrial materials. The relative importance of river input and coastal erosion varies among Arctic shelves in relation to spatial variability of sedimentary environment (Macdonald et al., 2015). However, little is known regarding the potential disparities in matrix-related biogeochemical behaviors of Hg input by these two distinct processes. In addition, the prolonged sea ice-free season and rising ocean temperature enhance the primary productivity and thereby its sequestration of Hg (Zaferani et al., 2018). This increases the uncertainty in the accurate assessment of the mass budget and source-to-sink process of Hg. Therefore, the objectives of the present study are: first, to uncover the disparities in mineral/organic matrix-related Hg sequestration and deposition resulting from spatial variability of input pathways; and second, to explore how primary productivity contributes to these disparities and the underlying mechanisms involved.

The East Siberian Arctic shelf (ESAS) is the largest shelf system in the world and comprises 40 % of the Arctic shelf, with remarkable spatial heterogeneity in contributions from riverine input, coastal erosion, and primary productivity. Therefore, the ESAS exhibits remarkable alongshore and offshore variabilities in THg concentration, OC sources, and sediment SSA (Fig. 1a, b, c). However, there are notable mismatches between the specific distribution of THg concentration and those of OC sources and sediment SSA (Fig. 1a, b, c). The varied distributions present an invaluable opportunity to investigate the role of organic and mineral matrices in Hg sequestration and deposition. Therefore, typical surface sediments from the ESAS were selected to identify the different behaviors and fates of Hg along the coastal area with distinct terrestrial inputs and marine primary productivity (Fig. 1d). Furthermore, we aimed to explore the underlying mechanisms in relation to the mineral and/or OC matrices for Hg sequestration in the Arctic marginal seas.

2. Materials and methods

2.1. Study area

The ESAS is the widest and shallowest continental shelf in the world, including the Laptev Sea (LS), East Siberian Sea (ESS), and Eurasian sector of Chukchi Sea (CS). The hydrologic catchment is dominated by continuous and discontinuous permafrost. Therefore, large amounts of OC and Hg stored in the permafrost are released into the shelf via riverine input and coastal erosion (Dastoor et al., 2022; McClelland et al., 2016; Vonk et al., 2012). The LS extends from ~110 to 140°E and covers an area of 500×10^3 km^2 with an average water depth of 50 m. It receives substantial amounts of terrestrial materials from the Lena River (Gordeev, 2006), which provides 20.7 Tg of suspended particulate matter (SPM), 0.8 Tg of particulate OC, 5.7 Tg of dissolved OC, and 6.6 Mg of Hg annually (Dastoor et al., 2022; Holmes et al., 2012; McClelland et al., 2016). Notably, the output fluxes of the terrestrial OC and Hg are the highest among the six major Arctic rivers. Due to the long coastal length and high erosion rate, the calculated Hg input from coastal erosion is up to 9.7 Mg yr^{-1}, but the LS off the Lena River mouth is mainly affected by the riverine input (Liem-Nguyen et al., 2022).

The ESS, spanning from 140°E to 180°E, is the largest marginal sea in the Arctic Ocean. This sea covers an area of 987×10^3 km^2 with an average water depth of 58 m and exhibits low bathymetric gradients. It exhibits two distinct biogeochemical regimes. The western ESS (WESS, 140°E to 160°E) experiences rapid coastal erosion at a rate of 3–4 m yr^{-1}(Lantuit et al., 2012), which releases substantial amount of OC from the Pleistocene ice complexes deposits (ICD) and contributes up to 4.4 Mg Hg to the WESS annually (Dastoor et al., 2022; Vonk et al., 2012). The eastern ESS (EESS, 160°E to 180°E) is influenced by the Pacific inflow waters and characterized by high primary productivity (Woodgate and Aagaard, 2005), which serves as an important source of OC (Martens et al., 2022). The riverine Hg input from the Kolyma River to the EESS is about 1.1 Mg yr^{-1}, and the Indigirka River is expected to contribute lower Hg flux into the WESS due to the low annual runoff (Dastoor et al., 2022).

The CS is located between the Alaska Peninsula, Chukchi Peninsula, and Wrangel Island, with a mean depth of 80 m (Jakobsson, 2002). It is connected to the North Pacific Ocean through the Bering Strait (Wang et al., 2023). The input of high-nutrient Pacific inflow waters leads to the highest primary productivity within the Arctic Ocean (Macdonald et al., 2015), with annual particulate primary production ranging from 20 to 400 g C m^{-2} yr^{-1} (Stein and Macdonald, 2004). Therefore, the marine phytoplankton serves as a crucial contribution to the OC pool.

Sediments within the shelves are transported by various mechanisms, including sea ice, dense near-bottom gravity flows, and ocean currents (Eicken et al., 1997; Wegner et al., 2013). The ocean flows are primarily influenced by prevailing large-scale atmospheric conditions, e.g., Arctic Oscillation (AO) (Darby et al., 2012). Specifically, during negative phase of the AO, the Transpolar Drift moves westward and the Lena River plume is transported across the shelf towards the Lomonosov Ridge. Conversely, during positive phase, the fresh water from the Lena River is carried along the coast towards the ESS and the Siberian Coastal Current is strengthened (Guay et al., 2001).

2.2. Sample collection and measurement

In the present study, typical surface sediment samples from the ESAS were selected with the original scientific concern of the matrix-based constraint on the behavior and fate of the sedimentary Hg as noted above. These sediment samples from the LS under the direct Lena River input as well as those with direct impact of coastal erosion were obtained during cruise LV77 and LV83 in summer 2016 and 2018, respectively (Fig. 1d). The samples were wrapped in pre-combusted aluminum foil immediately after collection and stored at 4 °C. Prior to chemical analysis, the samples were freeze-dried at −20 °C to effectively eliminate any moisture, ensuring accurate and reliable results.

The stable carbon isotope ($\delta^{13}C$) and lignin content of sediment samples from the LS transect and nearshore samples were firstly analyzed and reported in the present study. Briefly, the $\delta^{13}C$ analysis was performed on a Thermo Fisher 253 Plus mass spectrometer (Thermo Fisher Scientific, Waltham, MA, USA) with AEA-600 and USGS-40 standards after removal of carbonate with 1 M HCl. The $\delta^{13}C$ value was reported in ‰ relative to the international standard V-PDB and the standard deviations of duplicate samples were ± 0.3 %. Lignin phenols were analyzed using an alkaline CuO oxidation method. Samples were reacted with CuO and ferrous ammonium sulfate under oxygen-free alkaline conditions, then processed with recovery standards and extraction. After processing, samples were derivatized and analyzed by GC–MS. Qualitative and quantitative analyses were based on retention times and standard curves, using internal and external standards. Precision was 2–10 %.

2.3. Compilation of regional sedimentary data sets and statistical analysis

In order to present a large-scale occurrence of the sedimentary Hg and its matrix-based constrains with varied depositional settings, except the $\delta^{13}C$ and lignin contents in the LS as new input dataset in the present study, the data for the bulk OC, THg concentration, and part of the lignin phenols in the ESAS, as well as the circum-Arctic reported sedimentary Hg dataset, were also collected from previous publications (see details in Tables S1 and S2) (Canário et al., 2013; Chaudhary et al., 2022; Gobeil et al., 1999; Kim et al., 2020; Kohler et al., 2022; Liem-Nguyen et al., 2022; Sattarova et al., 2022; Yang et al., 2023; Ye et al., 2021; Zhang et al., 2023).

The data analyses were performed using SPSS software (version 25.0; IBM SPSS Institute, USA). Pearson correlation analysis was used to analyze the correlations between THg concentration and organic and mineral variables, including TOC, TN, TOC/TN, $\delta^{13}C$, lignin, median grain size (Md), and SSA. Then, partial correlation analyses were

performed to further explore whether THg concentration was directly controlled by TOC or SSA.

3. Results

3.1. Sedimentary OC and Hg in the coastal ESAS and pan-Arctic shelf seas

In the Arctic sediments, the THg concentrations were generally lower in the shelf area and higher in the deep-sea basin (Fig. 1a). For the shelf seas, the productive CS exhibited lower THg concentration compared to those areas affected by terrestrial inputs, with high THg concentrations mainly distributed in the river estuaries and outer shelves.

The two coastal regions of the LS and WESS exhibited highly different TOC and THg concentration (Fig. 2). Specifically, TOC values were lower in the coastal region of the WESS (averaging 0.68 %), in comparison to the higher TOC values detected in the coastal region of the LS (averaging 1.22 %). The THg concentration in the former region averaged 34 ng/g dw, with a maximum of 70 ng/g dw noted separately

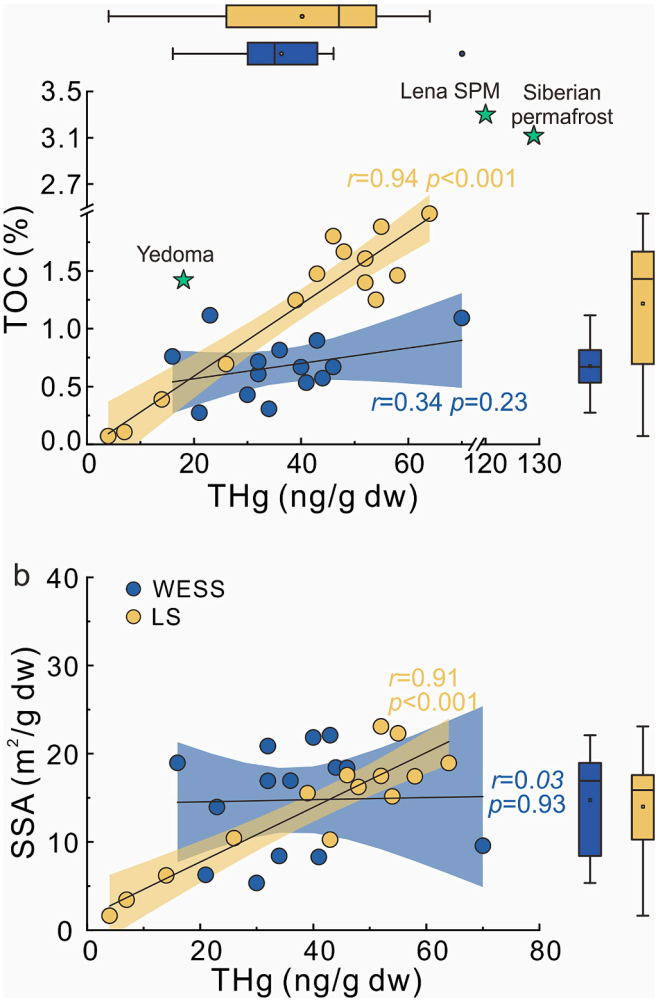

Fig. 2. Pearson correlation analyses of THg concentration with TOC (a) and SSA (b) in the LS and WESS coastal region (within a water depth of 30 m). The green stars represent endmembers for THg concentration and TOC in terrestrial provenance (Siberian permafrost (Zyrin et al., 1978) and ICD (Rutkowski et al., 2021)) and the Lena River SPM (Coquery et al., 1995). The box plots show the distribution (average, maximum, minimum, median, first and third quartiles) of THg concentration, TOC, and SSA values in each region. (For interpretation of the references to colour in this figure legend, the reader is referred to the web version of this article.)

(Fig. 2a), which was higher than that reported for the ICD (18 ng/g dw) (Rutkowski et al., 2021). The latter region exhibited a similar average THg concentration of 40 ng/g dw, which was lower than that of the Siberian permafrost (129 ng/g dw) (Zyrin et al., 1978) and the Lena River SPM (120 ng/g dw) (Coquery et al., 1995). These two regions exhibited similar SSA values, with 14.73 m^2/g dw and 13.97 m^2/g dw in the coastal regions of the WESS and LS, respectively (Fig. 2b). THg concentration exhibited varying correlations with TOC and SSA between these two regions (Fig. 2). In the coastal region of the LS, the THg concentration demonstrated significant positive correlations with both TOC ($r = 0.94$, $p < 0.001$) and SSA ($r = 0.91$, $p < 0.001$), whereas no significant correlations were observed in the coastal region of the WESS.

3.2. Hg deposition variation along two transects in the LS and WESS, and throughout the CS

Two transects extending towards the outer shelf were selected to examine the cross-shelf transportation and fate of terrestrial Hg in the context of riverine input and coastal erosion, respectively (Fig. 1d). Along the transect in the LS, THg concentration initially decreased from the mouth of the Lena River to the western New Siberian Islands and then gradually increased to the outer shelf, which was accompanied with corresponding variations in SSA, TOC, TOC/TN, $\delta^{13}C$, and lignin content (Fig. 3a). Pearson correlation analysis showed significant positive correlations between THg concentration and TOC ($r = 0.82$, $p < 0.001$), TN ($r = 0.96$, $p < 0.001$), and SSA ($r = 0.93$, $p < 0.001$), and a significant negative correlation with lignin content ($r = -0.75$, $p < 0.01$) (Fig. 4a). Despite the observed similarity in the variations of THg concentration, TOC/TN, and $\delta^{13}C$, there were no significant correlations between THg concentration and either TOC/TN ($r = -0.40$, $p = 0.17$) or $\delta^{13}C$ ($r = 0.21$, $p = 0.48$) throughout this transect (Fig. 4a).

A consistent increase in THg concentration was observed with increasing offshore distance along the WESS transect, paralleling the gradual increase in SSA (Fig. 3b). Simultaneously, $\delta^{13}C$ gradually increased while TOC/TN and lignin content progressively decreased. However, TOC only showed a slight reduction on the outer shelf. Pearson correlation analysis revealed significant correlations between THg concentration and both SSA ($r = 0.78$, $p < 0.01$), as well as source variables, including $\delta^{13}C$ ($r = 0.68$, $p < 0.05$), TOC/TN ($r = -0.86$, $p < 0.001$), TN ($r = 0.95$, $p < 0.001$), and lignin content ($r = -0.75$, $p < 0.01$) (Fig. 4b). However, no significant correlation was observed between THg concentration and TOC ($r = 0.48$, $p = 0.092$) (Fig. 4b).

Although the THg concentration in the CS was low, Pearson correlation analysis revealed significant positive correlations with TOC ($r = 0.94$, $p < 0.001$), TN ($r = 0.92$, $p < 0.001$), $\delta^{13}C$ ($r = 0.74$, $p < 0.05$), and SSA ($r = 0.90$, $p < 0.01$) (Fig. 4c). However, no significant correlations were observed with TOC/TN ($r = 0.46$, $p = 0.092$) or lignin ($r = 0.25$, $p = 0.092$). In addition, $\delta^{13}C$ and TN were significantly correlated with opal content with high correlation coefficients ($r = 0.82$, $p < 0.01$ and $r = 0.77$, $p < 0.05$, respectively).

4. Discussion

4.1. Controls of the spatial heterogeneity of Hg accumulation in coastal regions under varied input pathways

4.1.1. The role of organic/mineral matrices in Hg occurrence under riverine input

In order to further examine the matrix-related controls on the Hg sequestration, the partial correlation analysis was employed. The correlation between TOC and THg concentration remains significant even control the influence of SSA in the partial correlation analysis, whereas the reverse does not hold true (Fig. 5). This highlights the role of organic matrix in Hg sequestration, while the association between Hg and minerals may be mediated by OC.

In the LS, river runoff from the Lena River serves as the primary input

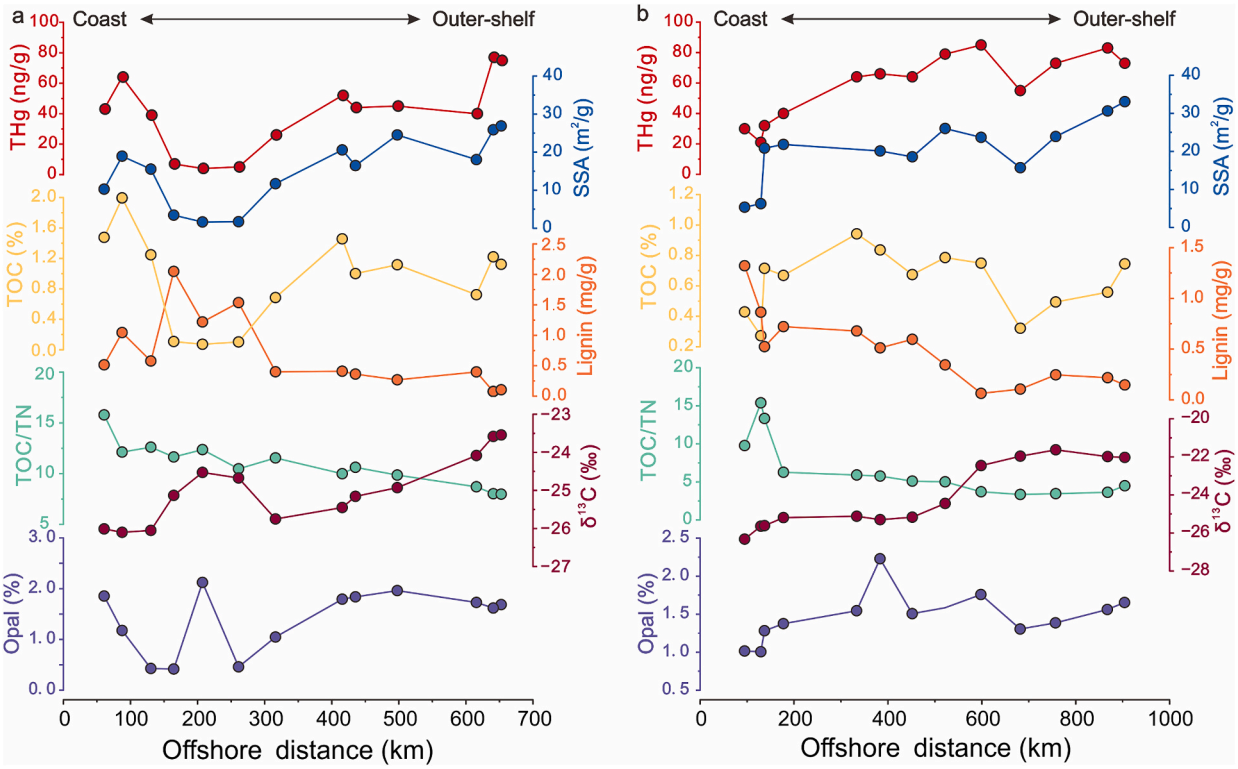

Fig. 3. Variations in levels of THg concentration, SSA, TOC, lignin, TOC/TN, $\delta^{13}C$, and opal with transport distance in the LS (a) and WESS (b). The details and origins of these data sets are summarized in Table S1.

pathway for Hg (Liem-Nguyen et al., 2022), with contributions from the thawing of permafrost (Lim et al., 2019; St Pierre et al., 2018) and melting snowpack during spring floods (Søndergaard et al., 2012). In the watershed permafrost, the Hg is usually proportional to the TOC content (Rydberg et al., 2010; Schuster et al., 2018; Schuster et al., 2011). This correlation is attributed to the fact that the uptake of atmospheric Hg(0) via vegetation and the subsequent litterfall accounts for approximately 55–73 % of Hg deposition and accumulation in the permafrost (Obrist et al., 2017), and the OC in permafrost has a strong affinity to and is normally complexed with Hg. Once the permafrost thaws, the OC-complexed Hg would be released into the river system as particulate Hg (Schuster et al., 2011), accounting for more than 60–90 % of the THg concentration in Arctic rivers (Søndergaard et al., 2015), and this proportion is increasing due to the widespread retrogressive thaw slumps in recent years (St Pierre et al., 2018). The Hg preserved in the snowpack, another important source of riverine Hg, is unlikely to be bound with OC. However, a study that examined the seasonal exports of Hg in the Yukon River revealed that the vast majority (90 %) of the exported Hg is complexed with particulate OC, regardless of whether the river water is sourced from snowmelt or thawing permafrost (Schuster et al., 2011). This can be attributable to the prolonged contact between Hg and matrices during fluvial processes (Kolka et al., 2001), which facilitates the sequestration of Hg by OC (Rhoton and Bennett, 2009). Therefore, initial-originated interactions between Hg and OC and/or those occur during subsequent riverine transportation determine that the fluvial-exported Hg is closely complexed with OC (Fig. 2a), as demonstrated by the positive correlation between Hg and OC in the SPM from Lena River estuary (Coquery et al., 1995; Grigal, 2002).

Fine-grained minerals (e.g., clay minerals and iron oxides) have strong affinity for contaminants and OC due to their high SSA and abundant reactive sites (Hu et al., 2023; Kleber et al., 2021). Therefore, the correlation between THg concentration and SSA has been widely reported in most mid- and low-latitude rivers and the adjacent continental margins (Chakraborty et al., 2014; Kim et al., 2018; Kongchum et al., 2011; Liu et al., 2017). However, the partial correlation results reveal that the mineral matrix may not directly sequestrate Hg, but rather mediated by OC. In permafrost, large amounts of OC are preserved by complexation with minerals (Martens et al., 2023; Szymański et al., 2022). Thus, the sequestration of Hg by OC during fluvial transit may facilitate the formation of mineral–OC–Hg complexes (Rhoton and Bennett, 2009).

4.1.2. *Accumulation of Hg in the WESS coastal region under erosion impact*

Coastal erosion, an abrupt process of permafrost degradation, leads to the rapid discharge of substantial quantities of previously frozen terrestrial materials, including Hg and OC, directly into the adjacent continental margins (Fritz et al., 2017). THg concentration is not significantly correlated with TOC and SSA in both Pearson and partial correlation analyses (Figs. 2 and 5), indicating no matrix-based constraint on Hg accumulation.

The current estimation of coastal erosion Hg export flux is based mainly on the THg concentration in permafrost soils (including active layers) and the eroding soil mass (Dastoor et al., 2022). In the WESS, however, the ICD constitute a significant proportion of the eroding sediments, surpassing those from active layers and permafrost. The ICD consists of OC-rich (1.2–4.8 %) and ice-rich (30–40 vol%) sediments with predominance of silts and fine sands (Schirrmeister et al., 2011; Strauss et al., 2013). The exposure of ICD in coastal high cliffs along WESS makes them more vulnerable and retreats 5–7 times faster than other coastal permafrost bodies (Lantuit et al., 2012), serving as the dominant source of terrestrial materials (Nielsen et al., 2022). However, the THg concentration is much lower in the ICD (18 ng/g) than in the active layers (65 ng/g) and permafrost (48 ng/g) (Dastoor et al., 2022; Rutkowski et al., 2021). Therefore, the low THg concentration in the sediment provenance determines that less THg is released into the WESS coastal region (Fig. 2a). Furthermore, the coastal-affected regions exhibits high sedimentation rates (Martens et al., 2022). Specifically, the WESS coastal region exhibits a mass accumulation rate of about 0.63 g

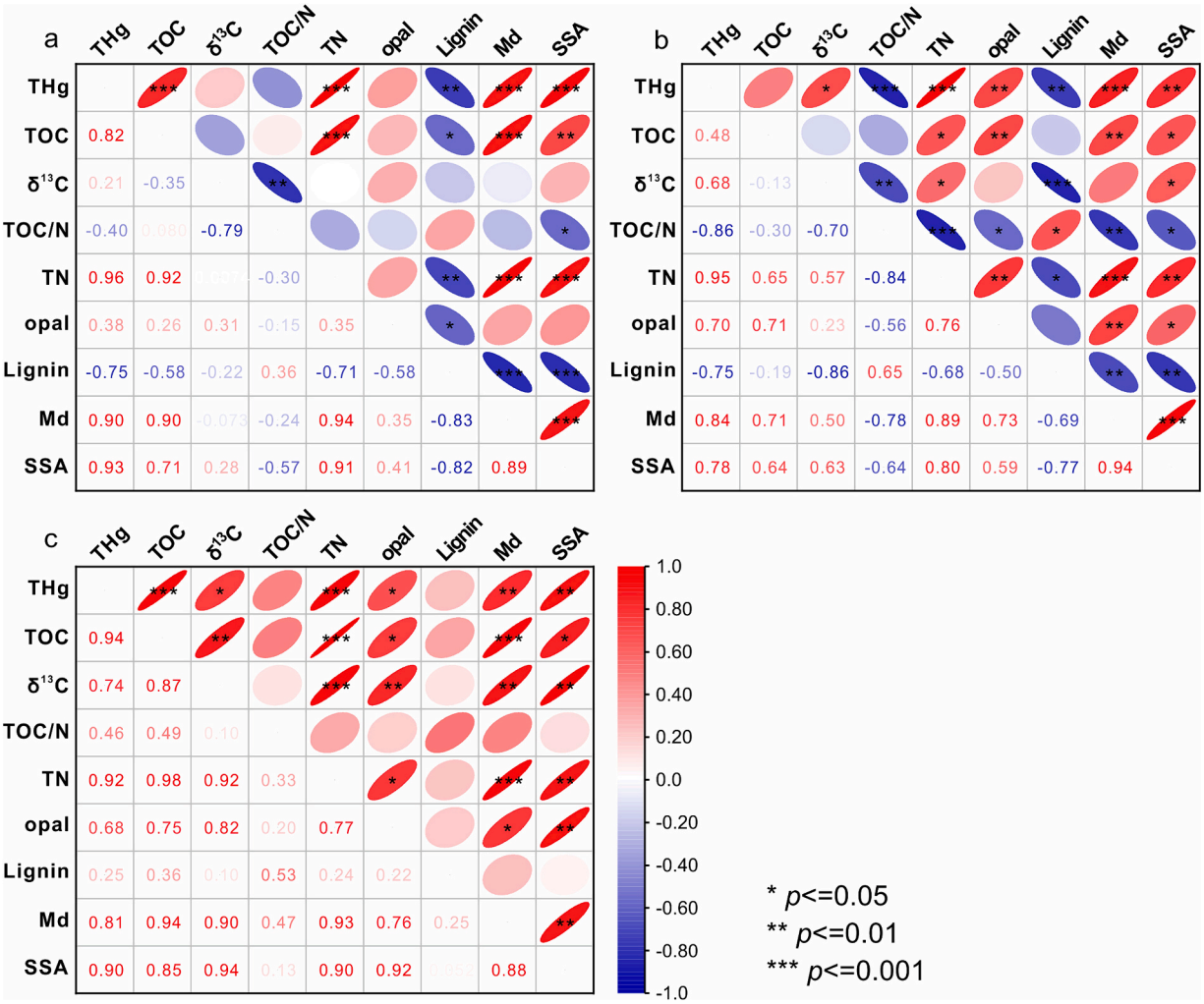

Fig. 4. Pearson correlation coefficient matrix heat map of (a) the LS transect, (b) WESS transect, and (c) the entire CS.

cm^{-2} yr^{-1}, which is approximately double that observed in the Lena River mouth regions (0.33 g cm^{-2} yr^{-1}) (Martens et al., 2022; Vonk et al., 2012). Deison et al. (2012) demonstrated that the rapid influx of inorganic materials can dilute the TOC and THg concentration in the sediments. The lower TOC in the WESS coastal sediments (0.68 %) compared to the ICD (1.2–4.8 %) confirms the dilution effect of high sedimentation rate on these THg concentration and OC in this coastal erosion-affected region.

The poor correlations between THg concentration and both TOC and SSA in the WESS coastal region (Figs. 2 and 5) are partially attributed to the inherently weak Hg complexation with OC and mineral matrices in the source ICD (Rutkowski et al., 2021). In addition, unlike riverine input, which provides long source-to-sink travel durations for Hg, the rapid and direct release of terrestrial materials through coastal erosion lacks these riverine loading processes, thereby limiting the adsorption of Hg onto OC and/or fine-grained sediments. Despite the capacity of OC and/or fine-grained sediments to sequestrate Hg during the sedimentation process (Rhoton and Bennett, 2009), the rapid sedimentation rate in the WESS coastal region may also hinder the sequestration effectiveness by restricting the temporal accessibility of Hg to the mineral and/or OC matrices.

4.2. *Matrix-related constraint on the fate of Hg in the ESAS*

4.2.1. *Cross-shelf behaviors of Hg deposition with mineral–OC–Hg complexes*

In the river-dominated LS, Hg is mainly complexed with OC and/or fine-grained sediments due to the modification of riverine processes. Once these terrestrial materials enter the marginal seas, both sediments and OC would be redistributed by hydrodynamic sorting (Tesi et al., 2016). Along the transect, the partial correlation coefficient between THg concentration and TOC (SSA) is still significant after removing the influence of SSA (TOC) in the partial correlation analyses (Fig. 5), indicating that deposition of Hg, present as OC–Hg and/or mineral–OC–Hg complexes, is also reshaped by the sediment transportation process under the hydrodynamic conditions (Liem-Nguyen et al., 2022). Meanwhile, despite the increasing dominance of marine OC with offshore distance, the consistent correlation between THg concentration and TOC suggests that the initially formed Hg–OC complexation would not be affected by the addition of fresh marine OC (Fig. 6).

4.2.2. *The role of marine OC in offshore Hg occurrence*

Along the WESS transect, the THg concentration is correlated with the OC source variables (e.g., $\delta^{13}C$ and lignin) rather than TOC (Fig. 4b), indicating the marine OC is more inclined to form complexes with Hg (Fig. 4). In addition, the enhancement of correlations between TOC and THg concentration after removing the correlation of $\delta^{13}C$ demonstrates that their poor correlation is greatly influenced by the distinct

LS coast	Control variables	TOC	SSA	$\delta^{13}C$
THg concentration	Zero-order	0.945***	0.915***	-0.059
	TOC		0.490	-0.047
	SSA	0.705**		0.009
	$\delta^{13}C$	0.944***	0.915***	

WESS coast	Control variables	TOC	SSA	$\delta^{13}C$
THg concentration	Zero-order	0.344	0.026	-0.344
	TOC		-0.142	-0.193
	SSA	0.369		-0.388
	$\delta^{13}C$	0.193	0.192	

LS transect	Control variables	TOC	SSA	$\delta^{13}C$
THg concentration	Zero-order	0.823***	0.926***	0.214
	TOC		0.855***	0.938***
	SSA	0.625*		-0.137
	$\delta^{13}C$	0.979***	0.924***	

WESS transect	Control variables	TOC	SSA	$\delta^{13}C$
THg concentration	Zero-order	0.482	0.781**	0.682**
	TOC		0.689*	0.855***
	SSA	0.016		0.442
	$\delta^{13}C$	0.774**	0.608*	

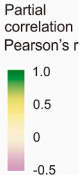

Fig. 5. Partial correlations of THg concentration with TOC, SSA, and $\delta^{13}C$ in the LS and WESS coast and transects. Numbers are the Pearson's r and the asterisks represent the strength of the correlation. * $p < 0.05$, ** $p < 0.01$, *** $p < 0.001$.

complexation ability of terrestrial OC and marine OC to Hg (Fig. 5).

We observed a negative correlation between THg concentration and lignin content (Fig. 4b), the latter being an essential component and tracer of terrestrial OC. Actually, complexation of Hg with OC typically occurs through chemical bonding between Hg(II) and specific functional groups. Oxygen-containing ligands, such as aldehyde, ketone, hydroxyl, and carboxyl groups, are the main functional groups within lignin (Pancost and Boot, 2004). The negative correlation indicates that these oxygen-containing ligands are not the primary adsorption sites for Hg, consistent with previous findings (Gerbig et al., 2011), and this typical terrestrial organic matter may have low affinity for Hg. However, the TN exhibits a positive correlation with THg (Fig. 4b). TN is mainly derived from nitrogen-containing ligands (e.g. amino groups) of amino acids and proteinaceous materials, which are widespread in the autogenous marine OC. The positive correlation between opal and TN confirms that the nitrogen-containing ligands are mainly derived from marine primary productivity (Fig. 4b). Adsorption experiments using Hg and biologically active amines showed that two amino groups can coordinate with one Hg(II), resulting in strong Hg–OC complexation (Ma et al., 2009; Misra et al., 1967; Peng et al., 2019). The greater correlation between TN and THg concentration compared to TOC indicates that the marine OC has stronger affinity for Hg than bulk OC (Chakraborty et al., 2015). This has also been widely observed in riverine suspended matter (Lim et al., 2019) and lacustrine sediments (Roulet et al., 2000).

Marine OC is dominant in the offshore region of the WESS, as indicated by the increase of $\delta^{13}C$ and decrease in TOC/TN. Phytoplankton blooms are widely observed along the sea ice edges when the melting nutrient-rich water is exposed to light (Lester et al., 2021). Under global warming, melting and thinning sea ice has allowed more light to penetrate the consolidated sea ice and promote the under-ice primary productivity (Ardyna et al., 2020; Arrigo et al., 2012; Payne et al., 2021). The upwelling along the shelf break would also cause phytoplankton blooms in the remote outer shelf (Jung et al., 2021). Therefore, the strong affinity of marine OC highlights the role of the biological pump in promoting Hg deposition in the outer shelf of the WESS (Fig. 6). The sequestration of Hg by mineral and/or OC matrices in sediments may serve as natural barrier to effectively reduce the generation of bioavailable methylmercury in the water column and its bioaccumulation in marine food webs (Zhang et al., 2015), thereby attenuating its biotoxicity and the threats of global warming to the Arctic and global ecosystems (Stern et al., 2012).

In the Chukchi Sea, where primary productivity is highest among the pan-Arctic seas (Hill et al., 2018; Zheng et al., 2021), the higher correlation coefficients of THg concentration with biogenic opal concentrations, $\delta^{13}C$ values, and TN demonstrate a greater enhancement of the regulatory effect of primary productivity on Hg deposition (Fig. 4c). However, although the sequestration of atmospheric Hg by primary productivity can promote the accumulation of Hg (Zaferani et al., 2018), the THg concentration is unexpectedly lower in the CS than the terrestrial-affected LS and ESS (Fig. 1a, Table S1). A recent Arctic Ocean Hg mass balance estimation suggested that the contributions of river runoff and coastal erosion (80 Mg yr^{-1}) exceed that of net atmospheric deposition (32 Mg yr^{-1}) (Dastoor et al., 2022). Therefore, the absence of direct riverine input and limited coastal erosion in the CS may restrict the available Hg for accumulation via the biological pump (Fig. 6). These findings highlight the synergy of terrestrial input and primary productivity in governing the deposition and fate of Hg in the ESAS.

4.3. Implications

Actually, the complexation of Hg and OC has been observed in the SPM in the Ob/Yenisei River-Kara Sea continuum (Coquery et al., 1995) and the Yukon River (Schuster et al., 2011). Furthermore, this phenomenon has also been widely found in the mid/low-latitude river and estuary-shelf continuum (Liu et al., 2017; Maurice-Bourgoin et al., 2003; Noh et al., 2013). Therefore, the mineral/organic matrix-related Hg sequestration and deposition have the potential to be extrapolated to other Arctic and mid/low latitude shelves that are predominantly influenced by riverine Hg inputs, which is benefit for re-evaluation of the biogeochemical behaviors and cycles of Hg. However, the effect of coastal erosion may vary significantly across regions, owing to the erosion rates and eroded materials across regions. For example, the American Arctic shelves exhibit generally lower coastal erosion rates and lacks the ICD (Lantuit et al., 2012). Therefore, further researches are needed to ascertain the matrix-related Hg sequestration in these erosion-dominated regions.

It is proposed that the in-situ methylation of Hg is normal in the Arctic shelf sediments (Kim et al., 2020), which is in relation to the OC matrices. Although the phytoplankton-derived OC can sequestrate the Hg via biological scavenging (Sanei and Goodarzi, 2006), these labile OC components are susceptible to microbial metabolism, thereby increasing microbial activity and potentially stimulating the methylation process (Lázaro et al., 2013). Conversely, the inert terrestrial OC, particularly that associated with minerals during the prolonged riverine loading process, remains recalcitrant to microbial degradation, thereby limiting microbial activity and the microbial methylation (Bravo et al., 2017). This implies that the tendency for methylation of Hg input via river and coastal erosion would differ, which is essential for assessing its

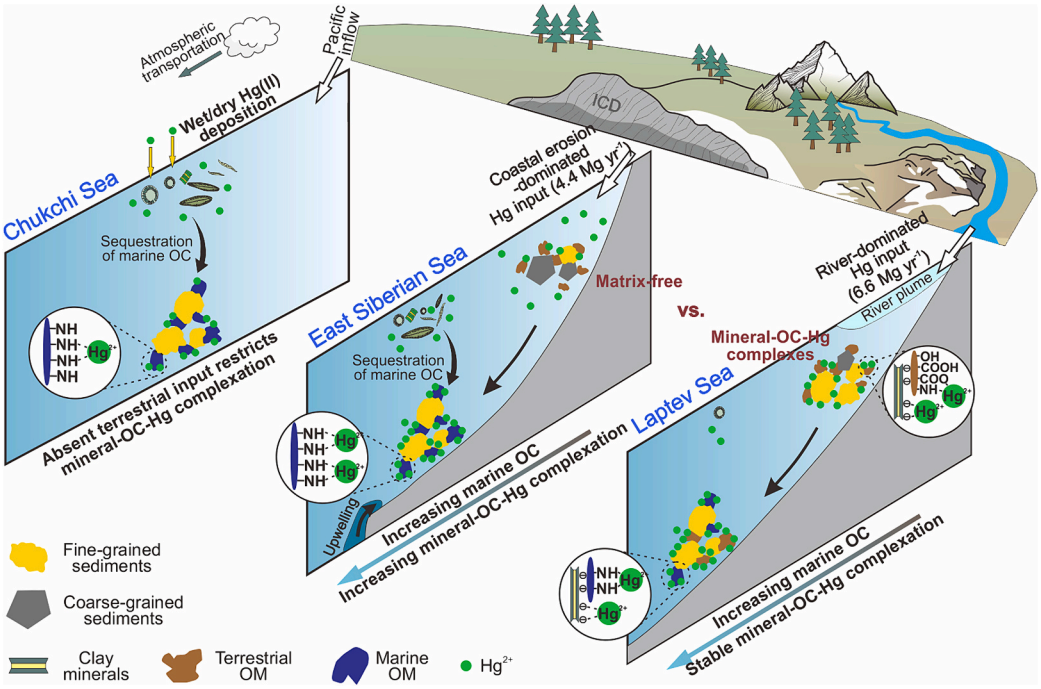

Fig. 6. Schematic illustration of Hg input and deposition heterogeneity in the ESAS. The riverine input Hg from the Lena River primarily enters the LS as mineral–OC–Hg complexes and remains stable during cross-shelf transportation. The Hg in the coastal erosion-affected region in WESS is present as matrix-free Hg and is deposited through complexation with marine OC in the high-primary productivity outer shelf. The high primary productivity in the CS enhances Hg complexation but the limited terrestrial input restricts its contribution to Hg deposition.

ecotoxicity and requires further exploration from the perspective of co-biogeochemical cycles of Hg and OC (Jonsson et al., 2022).

5. Conclusion

The terrestrial input pathways (riverine input vs. coastal erosion) are crucial in determining the mineral/organic matrix-related sequestration and deposition of Hg along the ESAS. In the river-dominated LS, the terrestrial Hg is exported and transported as mineral–OC–Hg complexes on the shelf, primarily due to the interactions of Hg with minerals and OC during the long-term fluvial sediment loading processes. Conversely, the rapid and direct release of terrestrial materials through coastal erosion in the WESS restricts the temporal accessibility of Hg for adsorption onto OC. With increasing offshore distance, the sequestration of Hg by autogenous marine OC in the high-primary productivity outer shelf enhances the deposition of Hg. However, despite the marked Hg complexations with marine OC in the CS, the THg concentration is unexpectedly low, indicating that scavenging by biological processes may be inadequate to sequestrate enough Hg in the CS. These findings highlight the synergistic effect of terrestrial input and biological processes in determining the varied deposition and fate of Hg in the ESAS.

CRediT authorship contribution statement

Jiazong Du: Visualization, Funding acquisition, Data curation, Conceptualization, Writing – review & editing, Writing – original draft. **Limin Hu:** Supervision, Funding acquisition, Writing – review & editing, Writing – original draft. **Zhengquan Yao:** Methodology, Data curation. **Yifang Sun:** Methodology, Data curation. **Gang Yang:** Methodology, Data curation. **Kirill Aksentov:** Investigation. **Yuriy Vasilenko:** Investigation. **Alexander Bosin:** Investigation. **Anatolii Astakhov:** Investigation. **Xuefa Shi:** Resources, Investigation. **Xiting Liu:** Writing – original draft.

Declaration of competing interest

The authors declare that they have no known competing financial interests or personal relationships that could have appeared to influence the work reported in this paper.

Data availability

Data will be made available on request.

Acknowledgement

This work was supported by the National Natural Science Foundation of China 42130412, 42076074, 42306064), Fundamental Research Funds for the Central Universities (Grant No. 202241001), National Key Research and Development Program of China (2023YFF0804600), China Postdoctoral Science Foundation (Grant No. 2023M743320). The expedition works were partly supported by the Ministry of Sciences and Higher Education of the Russian Federation (124022100083-1 and 124022100084-8).

Appendix A. Supplementary data

Supplementary data to this article can be found online at https://doi.org/10.1016/j.chemgeo.2024.122409.

References

Ardyna, M., Mundy, C.J., Mills, M.M., Oziel, L., Grondin, P.-L., Lacour, L., Verin, G., Dijken, G.V., Ras, J., Alou-Font, E., Babin, M., Gosselin, M., Tremblay, J.-É., Raimbault, P., Assmy, P., Nicolaus, M., Claustre, H., Arrigo, K.R., 2020. Environmental drivers of under-ice phytoplankton bloom dynamics in the Arctic Ocean. In: Elementa Science of the Anthropocene, 8, pp. 1–21. https://doi.org/10.1525/journal.elementa.430.

Arrigo, K.R., Perovich, D.K., Pickart, R.S., Brown, Z.W., Dijken, G.L.V., Lowry, K.E., Mills, M.M., Palmer, M.A., Balch, W.M., Bahr, F., Bates, N.R., Benitez-Nelson, C., Bowler, B., Brownlee, E., Ehn, J.K., Frey, K.E., Garley, R., Laney, S.R., Lubelczyk, L., Mathis, J., Matsuoka, A., Mitchell, B.G., Moore, G.W.K., Ortega-Retuerta, E., Pal, S.,

Polashenski, C.M., Reynolds, R.A., Schieber, B., Sosik, H.M., Stephens, M., Swift, J. H., 2012. Massive phytoplankton blooms under arctic sea ice. Science 336, 1408. https://doi.org/10.5061/dryad.4dn793t6.

Bravo, A.G., Bouchet, S., Tolu, J., Björn, E., Mateos-Rivera, A., Bertilsson, S., 2017. Molecular composition of organic matter controls methylmercury formation in boreal lakes. Nat. Commun. 8, 14255. https://doi.org/10.1038/ncomms14255.

Brigatti, M.F., Colonna, S., Malferrari, D., Medici, L., Poppi, L., 2005. Mercury adsorption by montmorillonite and vermiculite: a combined XRD, TG-MS, and EXAFS study. Appl. Clay Sci. 28, 1–8. https://doi.org/10.1016/j.clay.2004.03.006.

Canário, J., Poissant, L., Pilote, M., Blaise, C., Constant, P., Férard, J.-F., Gagné, F., 2013. Toxicity survey of Canadian Arctic marine sediments. J. Soils Sediments 14, 196–203. https://doi.org/10.1007/s11368-013-0792-1.

Chakraborty, P., Sharma, B., Babu, P.V., Yao, K.M., Jaychandran, S., 2014. Impact of total organic carbon (in sediments) and dissolved organic carbon (in overlying water column) on Hg sequestration by coastal sediments from the central east coast of India. Mar. Pollut. Bull. 79, 342–347. https://doi.org/10.1016/j.marpolbul.2013.11.028.

Chakraborty, P., Sarkar, A., Vudamala, K., Naik, R., Nath, B.N., 2015. Organic matter — a key factor in controlling mercury distribution in estuarine sediment. Mar. Chem. 173, 302–309. https://doi.org/10.1016/j.marchem.2014.10.005.

Chaudhary, D.K., Karki, H.P., Bajagain, R., Kim, H., Rhee, T.S., Hong, J.K., Han, S., Choi, Y.-G., Hong, Y., 2022. Mercury and other trace elements distribution and profiling of microbial community in the surface sediments of East Siberian Sea. Mar. Pollut. Bull. 185, 114319 https://doi.org/10.1016/j.marpolbul.2022.114319.

Coquery, M., Cossa, D., Martin, J.M., 1995. The distribution of dissolved and particulate mercury in three Siberian estuaries and adjacent Arctic coastal waters. Water Air Soil Pollut. 80, 653–664. https://doi.org/10.1007/BF01189718.

Darby, D.A., Ortiz, J.D., Grosch, C.E., Lund, S.P., 2012. 1,500-year cycle in the Arctic Oscillation identified in Holocene Arctic Sea-ice drift. Nat. Geosci. 5, 897–900. https://doi.org/10.1038/ngeo1629.

Dastoor, A., Angot, H., Bieser, J., Christensen, J.H., Douglas, T.A., Heimbürger-Boavida, L.-E., Jiskra, M., Mason, R.P., McLagan, D.S., Obrist, D., Outridge, P.M., Petrova, M.V., Ryjkov, A., St Pierre, K.A., Schartup, A.T., Soerensen, A.L., Toyota, K., Travnikov, O., Wilson, S.J., Zdanowicz, C., 2022. Arctic mercury cycling. Nat. Rev. Earth Environ. 3, 270–286. https://doi.org/10.1038/s43017-022-00269-w.

Deison, R., Smol, J.P., Kokelj, S.V., Pisaric, M.F.J., Kimpe, L.E., Poulain, A.J., Sanei, H., Thienpont, J.R., Blais, J.M., 2012. Spatial and Temporal Assessment of Mercury and Organic Matter in Thermokarst Affected Lakes of the Mackenzie Delta Uplands, NT, Canada. Environ. Sci. Technol. 46, 8748–8755. https://doi.org/10.1021/es300798w.

Durnford, D., Dastoor, A., Figueras-Nieto, D., Ryjkov, A., 2010. Long range transport of mercury to the Arctic and across Canada. Atmos. Chem. Phys. 10, 6063–6086. https://doi.org/10.5194/acp-10-6063-2010.

Eicken, H., Reimnitz, E., Alexandrov, V., Martin, T., Kassens, H., Viehoff, T., 1997. Sea-ice processes in the Laptev Sea and their importance for sediment export. Cont. Shelf Res. 17, 205–233. https://doi.org/10.1016/S0278-4343(96)00024-6.

Fisher, J.A., Jacob, D.J., Soerensen, A.L., Amos, H.M., Steffen, A., Sunderland, E.M., 2012. Riverine source of Arctic Ocean mercury inferred from atmospheric observations. Nat. Geosci. 5, 499–504. https://doi.org/10.1038/ngeo1478.

Fritz, M., Vonk, J.E., Lantuit, H., 2017. Collapsing Arctic coastlines. Nat. Clim. Chang. 7, 6–7. https://doi.org/10.1038/nclimate3188.

Gerbig, C.A., Ryan, J.N., Aiken, G.R., 2011. The Effects of Dissolved Organic Matter on Mercury Biogeochemistry. In: Liu, G., Cai, Y., O'Driscoll, N. (Eds.), Environmental Chemistry and Toxicology of Mercury. Wiley & Sons, Hoboken, Ner Jersey, pp. 259–292.

Gobeil, C., Macdonald, R.W., Smith, J.N., 1999. Mercury profiles in sediments of the arctic ocean basins. Environ. Sci. Technol. 33, 4194–4198.

Gordeev, V.V., 2006. Fluvial sediment flux to the Arctic Ocean. Geomorphology 80, 94–104. https://doi.org/10.1016/j.geomorph.2005.09.008.

Grigal, D.F., 2002. Inputs and outputs of mercury from terrestrial watersheds a review. Environ. Rev. 10, 1–39. https://doi.org/10.1139/A01-013.

Guay, C.K.H., Falkner, K.K., Muench, R.D., Mensch, M., Frank, M., Bayer, R., 2001. Wind-driven transport pathways for Eurasian Arctic river discharge. J. Geophys. Res. Oceans 106, 11469–11480. https://doi.org/10.1029/2000jc000261.

Hammerschmidt, C.R., Fitzgerald, W.F., 2004. Geochemical Controls on the production and distribution of Methylmercury in Near-Shore Marine Sediments. Environ. Sci. Technol. 38, 1487–1495. https://doi.org/10.1021/es034528q.

Hill, V., Ardyna, M., Lee, S.H., Varela, D.E., 2018. Decadal trends in phytoplankton production in the Pacific Arctic Region from 1950 to 2012. Deep-Sea Res. II Top. Stud. Oceanogr. 152, 82–94. https://doi.org/10.1016/j.dsr2.2016.12.015.

Holmes, R.M., McClelland, J.W., Peterson, B.J., Tank, S.E., Bulygina, E., Eglinton, T.I., Gordeev, V.V., Gurtovaya, T.Y., Raymond, P.A., Repeta, D.J., Staples, R., Striegl, R. G., Zhulidov, A.V., Zimov, S.A., 2012. Seasonal and Annual Fluxes of Nutrients and Organic Matter from large Rivers to the Arctic Ocean and Surrounding Seas. Estuar. Coasts 35, 369–382. https://doi.org/10.1007/s12237-011-9386-6.

Hu, L., Ji, Y., Zhao, B., Liu, X., Du, J., Liang, Y., Yao, P., 2023. The effect of iron on the preservation of organic carbon in marine sediments and its implications for carbon sequestration. Sci. China Earth Sci. 66, 1946–1959. https://doi.org/10.1007/s11430-023-1139-9.

Jakobsson, M., 2002. Hypsometry and volume of the Arctic Ocean and its constituent seas. Geochem. Geophys. Geosyst. 3, 1–18. https://doi.org/10.1029/2001gc000302.

Jonsson, S., Mastromonaco, M.N., Wang, F., Bravo, A.G., Cairns, W.R.L., Chételat, J., Douglas, T.A., Lescord, G., Ukonmaanaho, L., Heimbürger-Boavida, L.-E., 2022. Arctic methylmercury cycling. Sci. Total Environ. 850, 157445 https://doi.org/10.1016/j.scitotenv.2022.157445.

Jung, J., Cho, K.H., Park, T., Yoshizawa, E., Lee, Y., Yang, E.J., Gal, J.K., Ha, S.Y., Kim, S., Kang, S.H., Grebmeier, J.M., 2021. Atlantic-Origin Cold Saline Water Intrusion and Shoaling of the Nutricline in the Pacific Arctic. Geophys. Res. Lett. 48 https://doi.org/10.1029/2020gl090907 e2020GL090907.

Kehrig, H.A., Pinto, F.N., Moreira, I., Malm, O., 2003. Heavy metals and methylmercury in a tropical coastal estuary and a mangrove in Brazil. Org. Geochem. 34, 661–669. https://doi.org/10.1016/s0146-6380(03)00021-4.

Kim, J., Lim, D., Jung, D., Kang, J., Jung, H., Woo, H., Jeong, K., Xu, Z., 2018. Sedimentary mercury (Hg) in the marginal seas adjacent to Chinese high-Hg emissions: Source-to-sink, mass inventory, and accumulation history. Mar. Pollut. Bull. 128, 428–437. https://doi.org/10.1016/j.marpolbul.2018.01.058.

Kim, J., Soerensen, A.L., Kim, M.S., Eom, S., Rhee, T.S., Jin, Y.K., Han, S., 2020. Mass Budget of Methylmercury in the East Siberian Sea: the Importance of Sediment sources. Environ. Sci. Technol. 54, 9949–9957. https://doi.org/10.1021/acs.est.0c00154.

Kim, D.V., Sattarova, V.V., Aksentov, K.I., Lopatnikov, E.A., Ivanov, M.V., Alatortsev, A. V., Melgunov, M.S., 2023. Mercury geochemistry of marine sediments from the eastern Laptev Sea: the spatial distribution, levels, and contamination assessment. Mar. Pollut. Bull. 187, 114576 https://doi.org/10.1016/j.marpolbul.2023.114576.

Kleber, M., Bourg, I.C., Coward, E.K., Hansel, C.M., Myneni, S.C.B., Nunan, N., 2021. Dynamic interactions at the mineral–organic matter interface. Nat. Rev. Earth Environ. 2, 402–421. https://doi.org/10.1038/s43017-021-00162-y.

Kohler, S.G., Kull, L.M., Heimbürger-Boavida, L.-E., Ricardo de Freitas, T., Sanchez, N., Ndungu, K., Ardelan, M.V., 2022. Distribution pattern of mercury in northern Barents Sea and Eurasian Basin surface sediment. Mar. Pollut. Bull. 185, 114272 https://doi.org/10.1016/j.marpolbul.2022.114272.

Kolka, R.K., Grigal, D.F., Nater, E.A., Verry, E.S., 2001. Hydrologic cycling of mercury and organic carbon in a forested Upland–Bog Watershed. Soil Sci. Soc. Am. J. 65, 897–905. https://doi.org/10.2136/sssaj2001.653897x.

Kongchum, M., Hudnall, W.H., DeLaune, R.D., 2011. Relationship between sediment clay minerals and total mercury. J. Environ. Sci. Health A Tox. Hazard. Subst. Environ. Eng. 46, 534–539. https://doi.org/10.1080/10934529.2011.551745.

Lantuit, H., Overduin, P.P., Couture, N., Wetterich, S., Aré, F., Atkinson, D., Brown, J., Cherkashov, G., Drozdov, D., Forbes, D.L., Graves-Gaylord, A., Grigoriev, M., Hubberten, H.-W., Jordan, J., Jorgenson, T., Ødegård, R.S., Ogorodov, S., Pollard, W. H., Rachold, V., Sedenko, S., Solomon, S., Steenhuisen, F., Streletskaya, I., Vasiliev, A., 2012. The Arctic Coastal Dynamics Database: a New Classification Scheme and Statistics on Arctic Permafrost Coastlines. Estuar. Coasts 35, 383–400. https://doi.org/10.1007/s12237-010-9362-6.

Lázaro, W.L., Guimarães, J.R.D., Ignácio, A.R.A., Da Silva, C.J., Díez, S., 2013. Cyanobacteria enhance methylmercury production: a hypothesis tested in the periphyton of two lakes in the Pantanal floodplain, Brazil. Sci. Total Environ. 456-457, 231–238. https://doi.org/10.1016/j.scitotenv.2013.03.022.

Lester, C.W., Wagner, T.J.W., McNamara, D.E., Cape, M.R., 2021. The Influence of Meltwater on Phytoplankton Blooms near the Sea-Ice Edge. Geophys. Res. Lett. 48 https://doi.org/10.1029/2020gl091758 e2020GL091758.

Liem-Nguyen, V., Wild, B., Gustafsson, Ö., Semiletov, I., Dudarev, O., Jonsson, S., 2022. Spatial patterns and distributional controls of total and methylated mercury off the Lena River in the Laptev Sea sediments. Mar. Chem. 238, 104052 https://doi.org/10.1016/j.marchem.2021.104052.

Lim, A.G., Sonke, J.E., Krickov, I.V., Manasypov, R.M., Loiko, S.V., Pokrovsky, O.S., 2019. Enhanced particulate Hg export at the permafrost boundary, western Siberia. Environ. Pollut. 254, 113083 https://doi.org/10.1016/j.envpol.2019.113083.

Lim, A.G., Jiskra, M., Sonke, J.E., Loiko, S.V., Kosykh, N., Pokrovsky, O.S., 2020. A revised pan-Arctic permafrost soil Hg pool based on Western Siberian peat Hg and carbon observations. Biogeosciences 17, 3083–3097. https://doi.org/10.5194/bg-17-3083-2020.

Liu, W., Hu, L., Lin, T., Li, Y., Guo, Z., 2017. Distribution and mass inventory of mercury in sediment from the Yangtze River estuarine-inner shelf of the East China Sea. Cont. Shelf Res. 132, 29–37. https://doi.org/10.1016/j.csr.2016.11.004.

Ma, N., Yang, Y., Chen, S., Zhang, Q., 2009. Preparation of amine group-containing chelating fiber for thorough removal of mercury ions. J. Hazard. Mater. 171, 288–293. https://doi.org/10.1016/j.jhazmat.2009.06.001.

Macdonald, R.W., Kuzyk, Z.Z.A., Johannessen, S.C., 2015. The vulnerability of Arctic shelf sediments to climate change. Environ. Rev. 23, 461–479. https://doi.org/10.1139/er-2015-0040.

Martens, J., Romankevich, E., Semiletov, I., Wild, B., van Dongen, B., Vonk, J., Tesi, T., Shakhova, N., Dudarev, O.V., Kosmach, D., Vetrov, A., Lobkovsky, L., Belyaev, N., Macdonald, R.W., Pieńkowski, A.J., Eglinton, T.I., Haghipour, N., Dahle, S., Carroll, M.L., Åström, E.K.L., Grebmeier, J.M., Cooper, L.W., Possnert, G., Gustafsson, Ö., 2021. CASCADE – the Circum-Arctic Sediment CArbon DatabasE. Earth Syst. Sci. Data 13, 2561–2572. https://doi.org/10.5194/essd-13-2561-2021.

Martens, J., Wild, B., Semiletov, I., Dudarev, O.V., Gustafsson, O., 2022. Circum-Arctic release of terrestrial carbon varies between regions and sources. Nat. Commun. 13, 5858. https://doi.org/10.1038/s41467-022-33541-0.

Martens, J., Mueller, C.W., Joshi, P., Rosinger, C., Maisch, M., Kappler, A., Bonkowski, M., Schwamborn, G., Schirrmeister, L., Rethemeyer, J., 2023. Stabilization of mineral-associated organic carbon in Pleistocene permafrost. Nat. Commun. 14, 2120. https://doi.org/10.1038/s41467-023-37766-5.

Mason, R.P., Lawrence, A.L., 1999. Concentration, distribution, and bioavailability of mercury and methylmercury in sediments of Baltimore Harbor and Chesapeake Bay, Maryland, USA. Environ. Toxicol. Chem. 18, 2438–2447. https://doi.org/10.1002/etc.5620181109.

Maurice-Bourgoin, L., Quemerais, B., Moreira-Turcq, P., Seyler, P., 2003. Transport, distribution and speciation of mercury in the Amazon River at the confluence of

black and white waters of the Negro and Solimões Rivers. Hydrol. Process. 17, 1405–1417. https://doi.org/10.1002/hyp.1292.
McClelland, J.W., Holmes, R.M., Peterson, B.J., Raymond, P.A., Striegl, R.G., Zhulidov, A.V., Zimov, S.A., Zimov, N., Tank, S.E., Spencer, R.G.M., Staples, R., Gurtovaya, T.Y., Griffin, C.G., 2016. Particulate organic carbon and nitrogen export from major Arctic rivers. Glob. Biogeochem. Cycles 30, 629–643. https://doi.org/10.1002/2015gb005351.
Misra, C.H., Parmar, S.S., Shukla, S.N., 1967. Studies on complex compounds. V. Coordination compounds of mercury and biologically active amines. Can. J. Chem. 46, 2685–2691. https://doi.org/10.1139/v68-442.
Nielsen, D.M., Pieper, P., Barkhordarian, A., Overduin, P., Ilyina, T., Brovkin, V., Baehr, J., Dobrynin, M., 2022. Increase in Arctic coastal erosion and its sensitivity to warming in the twenty-first century. Nat. Clim. Chang. 12, 263–270. https://doi.org/10.1038/s41558-022-01281-0.
Noh, S., Choi, M., Kim, E., Dan, N.P., Thanh, B.X., Ha, N.T.V., Sthiannopkao, S., Han, S., 2013. Influence of salinity intrusion on the speciation and partitioning of mercury in the Mekong River Delta. Geochim. Cosmochim. Acta 106, 379–390. https://doi.org/10.1016/j.gca.2012.12.018.
Obrist, D., Agnan, Y., Jiskra, M., Olson, C.L., Colegrove, D.P., Hueber, J., Moore, C.W., Sonke, J.E., Helmig, D., 2017. Tundra uptake of atmospheric elemental mercury drives Arctic mercury pollution. Nature 547, 201–204. https://doi.org/10.1038/nature22997.
Pancost, R.D., Boot, C.S., 2004. The palaeoclimatic utility of terrestrial biomarkers in marine sediments. Mar. Chem. 92, 239–261. https://doi.org/10.1016/j.marchem.2004.06.029.
Park, J.-H., Wang, J.J., Xiao, R., Pensky, S.M., Kongchum, M., DeLaune, R.D., Seo, D.-C., 2018. Mercury adsorption in the Mississippi River deltaic plain freshwater marsh soil of Louisiana Gulf coastal wetlands. Chemosphere 195, 455–462. https://doi.org/10.1016/j.chemosphere.2017.12.104.
Payne, C.M., Bianucci, L., van Dijken, G.L., Arrigo, K.R., 2021. Changes in Under-Ice primary production in the Chukchi Sea from 1988 to 2018. J. Geophys. Res. Oceans 126. https://doi.org/10.1029/2021jc017483 e2021JC017483.
Peng, R., Chen, G., Zhou, F., Man, R., Huang, J., 2019. Catalyst-free synthesis of triazine-based porous organic polymers for Hg2+ adsorptive removal from aqueous solution. Chem. Eng. J. 371, 260–266. https://doi.org/10.1016/j.cej.2019.04.063.
Phothitontimongkol, T., Siebers, N., Sukpirom, N., Unob, F., 2009. Preparation and characterization of novel organo-clay minerals for Hg(II) ions adsorption from aqueous solution. Appl. Clay Sci. 43, 343–349. https://doi.org/10.1016/j.clay.2008.09.016.
Rachold, V., Eicken, H., Gordeev, V.V., Grigoriev, M.N., Hubberten, H.-W., Lisitzin, A.P., Shevchenko, V.P., Schirrmeister, L., 2004. Modern terrigenous organic carbon input to the Arctic Ocean. In: Stein, R., Macdonald, R.W. (Eds.), The Organic Carbon Cycle in the Arctic Ocean. Springer-Verlag, Berlin Heidelberg, pp. 33–55.
Ravichandran, M., 2004. Interactions between mercury and dissolved organic matter–a review. Chemosphere 55, 319–331. https://doi.org/10.1016/j.chemosphere.2003.11.011.
Rhoton, F.E., Bennett, S.J., 2009. Soil and sediment properties affecting the accumulation of mercury in a flood control reservoir. Catena 79, 39–48. https://doi.org/10.1016/j.catena.2009.05.004.
Roulet, M., Lucotte, M., Canuel, R., Farella, N., Courcelles, M., Guimarães, J.-R.D., Mergler, D., Amorim, M., 2000. Increase in mercury concentration recorded in lacustrian sediments following deforestation in Central Amazon. Chem. Geol. 165, 243–266.
Rutkowski, C., Lenz, J., Lang, A., Wolter, J., Mothes, S., Reemtsma, T., Grosse, G., Ulrich, M., Fuchs, M., Schirrmeister, L., Fedorov, A., Grigoriev, M., Lantuit, H., Strauss, J., 2021. Mercury in sediment core samples from Deep Siberian Ice-Rich Permafrost. Front. Earth Sci. 9, 718153 https://doi.org/10.3389/feart.2021.718153.
Rydberg, J., Klaminder, J., Rosen, P., Bindler, R., 2010. Climate driven release of carbon and mercury from permafrost mires increases mercury loading to sub-arctic lakes. Sci. Total Environ. 408, 4778–4783. https://doi.org/10.1016/j.scitotenv.2010.06.056.
Sanei, H., Goodarzi, F., 2006. Relationship between organic matter and mercury in recent lake sediment: the physical–geochemical aspects. Appl. Geochem. 21, 1900–1912. https://doi.org/10.1016/j.apgeochem.2006.08.015.
Sanei, H., Grasby, S.E., Beauchamp, B., 2011. Latest Permian mercury anomalies. Geology 40, 63–66. https://doi.org/10.1130/g32596.1.
Sattarova, V.V., Aksentov, K.I., Ivanov, M.V., Alatortsev, A.V., Kim, D.V., Obrezkova, M. S., 2022. Distribution and assessment of trace metals in modern bottom sediments in the southwestern Chukchi Sea. Mar. Pollut. Bull. 180, 113797 https://doi.org/10.1016/j.marpolbul.2022.113797.
Schirrmeister, L., Kunitsky, V., Grosse, G., Wetterich, S., Meyer, H., Schwamborn, G., Babiy, O., Derevyagin, A., Siegert, C., 2011. Sedimentary characteristics and origin of the late Pleistocene Ice complex on north-east Siberian Arctic coastal lowlands and islands – a review. Quat. Int. 241, 3–25. https://doi.org/10.1016/j.quaint.2010.04.004.
Schuster, P.F., Striegl, R.G., Aiken, G.R., Krabbenhoft, D.P., Dewild, J.F., Butler, K., Kamark, B., Dornblaser, M., 2011. Mercury export from the Yukon River Basin and potential response to a changing climate. Environ. Sci. Technol. 45, 9262–9267. https://doi.org/10.1021/es202068b.
Schuster, P.F., Schaefer, K.M., Aiken, G.R., Antweiler, R.C., Dewild, J.F., Gryziec, J.D., Gusmeroli, A., Hugelius, G., Jafarov, E., Krabbenhoft, D.P., Liu, L., Herman-Mercer, N., Mu, C., Roth, D.A., Schaefer, T., Striegl, R.G., Wickland, K.P., Zhang, T., 2018. Permafrost Stores a Globally significant Amount of Mercury. Geophys. Res. Lett. 45, 1463–1471. https://doi.org/10.1002/2017gl075571.
Søndergaard, J., Rigét, F., Tamstorf, M.P., Larsen, M.M., 2012. Mercury transport in a Low-Arctic River in Kobbefjord, West Greenland (64° N). Water Air Soil Pollut. 223, 4333–4342. https://doi.org/10.1007/s11270-012-1198-1.
Søndergaard, J., Tamstorf, M., Elberling, B., Larsen, M.M., Mylius, M.R., Lund, M., Abermann, J., Riget, F., 2015. Mercury exports from a High-Arctic river basin in Northeast Greenland (74 degrees N) largely controlled by glacial lake outburst floods. Sci. Total Environ. 514, 83–91. https://doi.org/10.1016/j.scitotenv.2015.01.097.
St Pierre, K.A., Zolkos, S., Shakil, S., Tank, S.E., St Louis, V.L., Kokelj, S.V., 2018. Unprecedented increases in Total and Methyl Mercury Concentrations Downstream of Retrogressive Thaw Slumps in the Western Canadian Arctic. Environ. Sci. Technol. 52, 14099–14109. https://doi.org/10.1021/acs.est.8b05348.
Stein, R., Macdonald, R.W., 2004. The Organic Carbon Cycle in the Arctic Ocean. Springer-Verlag, Berlin.
Stern, G.A., Sanei, H., Roach, P., Delaronde, J., Outridge, P.M., 2009. Historical Interrelated Variations of Mercury and Aquatic Organic Matter in Lake Sediment Cores from a Subarctic Lake in Yukon, Canada: further evidence toward the Algal-Mercury Scavenging Hypothesis. Environ. Sci. Technol. 43, 7684–7690. https://doi.org/10.1021/es902186s.
Stern, G.A., Macdonald, R.W., Outridge, P.M., Wilson, S., Chételat, J., Cole, A., Hintelmann, H., Loseto, L.L., Steffen, A., Wang, F., Zdanowicz, C., 2012. How does climate change influence arctic mercury? Sci. Total Environ. 414, 22–42. https://doi.org/10.1016/j.scitotenv.2011.10.039.
Stoichev, T., Amouroux, D., Wasserman, J.C., Point, D., De Diego, A., Bareille, G., Donard, O.F.X., 2004. Dynamics of mercury species in surface sediments of a macrotidal estuarine–coastal system (Adour River, Bay of Biscay). Estuar. Coast. Shelf Sci. 59, 511–521. https://doi.org/10.1016/j.ecss.2003.10.007.
Strauss, J., Schirrmeister, L., Grosse, G., Wetterich, S., Ulrich, M., Herzschuh, U., Hubberten, H.W., 2013. The deep permafrost carbon pool of the Yedoma region in Siberia and Alaska. Geophys. Res. Lett. 40, 6165–6170. https://doi.org/10.1002/2013GL058088.
Sun, X., Hu, L., Sun, X., Fan, D., Liu, M., Wang, H., Yang, Z., Cheng, P., Liu, X., Guo, Z., 2023. Mercury Burial in Modern Sedimentary Systems of the East China Marginal Seas: the Role of Coastal Oceans in Global Mercury Cycling. Glob. Biogeochem. Cycles 37. https://doi.org/10.1029/2023gb007760 e2023GB007760.
Szymański, W., Drewnik, M., Stolarczyk, M., Musielok, Ł., Gus-Stolarczyk, M., Skiba, M., 2022. Occurrence and stability of organic intercalation in clay minerals from permafrost-affected soils in the High Arctic – a case study from Spitsbergen (Svalbard). Geoderma 408, 115591. https://doi.org/10.1016/j.geoderma.2021.115591.
Tesi, T., Semiletov, I., Dudarev, O., Andersson, A., Gustafsson, Ö., 2016. Matrix association effects on hydrodynamic sorting and degradation of terrestrial organic matter during cross-shelf transport in the Laptev and East Siberian shelf seas. J. Geophys. Res. Biogeosci. 121, 731–752. https://doi.org/10.1002/2015jg003067.
Vonk, J.E., Sanchez-Garcia, L., van Dongen, B.E., Alling, V., Kosmach, D., Charkin, A., Semiletov, I.P., Dudarev, O.V., Shakhova, N., Roos, P., Eglinton, T.I., Andersson, A., Gustafsson, O., 2012. Activation of old carbon by erosion of coastal and subsea permafrost in Arctic Siberia. Nature 489, 137–140. https://doi.org/10.1038/nature11392.
Wang, Q., Shu, Q., Wang, S., Beszczynska-Moeller, A., Danilov, S., Steur, L., Haine, T.W. N., Karcher, M., Lee, C.M., Myers, P.G., Polyakov, I.V., Provost, C., Skagseth, Ø., Spreen, G., Woodgate, R., 2023. A review of Arctic–Subarctic Ocean Linkages: past changes, mechanisms, and future projections. Ocean-Land-Atmos. Res. 2, 0013. https://doi.org/10.34133/olar.0013.
Wegner, C., Bauch, D., Hölemann, J.A., Janout, M.A., Heim, B., Novikhin, A., Kassens, H., Timokhov, L., 2013. Interannual variability of surface and bottom sediment transport on the Laptev Sea shelf during summer. Biogeosciences 10, 1117–1129. https://doi.org/10.5194/bg-10-1117-2013.
Woodgate, R.A., Aagaard, K., 2005. Revising the Bering Strait freshwater flux into the Arctic Ocean. Geophys. Res. Lett. 32 https://doi.org/10.1029/2004gl021747.
Wu, F., Xu, L., Liao, H., Guo, F., Zhao, X., Giesy, J.P., 2013. Relationship between mercury and organic carbon in sediment cores from Lakes Qinghai and Chenghai, China. J. Soils Sediments 13, 1084–1092. https://doi.org/10.1007/s11368-013-0694-2.
Yang, G., Yao, Z., Feng, H., Hu, L., Anatolii, A., Zou, J., Liu, Y., Wang, K., Alexander, B., Yuri, V., Yang, G., Shi, X., 2023. Distribution characteristics and environmental significance of biogenic silica in the surface sediments of the Arctic East Siberian Shelf. Bull. Mineral. Petrol. Geochem. 42, 717–727. https://doi.org/10.19658/j.issn.1007-2802.2023.42.105.
Ye, J., Hu, L., Shi, X., Yao, P., Xia, Y., Bai, Y., Zhang, Y., 2021. Sources, transport and burial of terrestrial organic carbon in the surface sediments across the East Siberian Arctic Shelf, insight from lignin. Quater. Sci. 41, 752–765. https://doi.org/10.11928/j.issn.1001-7410.2021.03.11.
Zaferani, S., Pérez-Rodríguez, M., Biester, H., 2018. Diatom ooze—a large marine mercury sink. Science 361, 797–800. https://doi.org/10.1126/science.aat2735.
Zhang, Y., Jacob, D.J., Dutkiewicz, S., Amos, H.M., Long, M.S., Sunderland, E.M., 2015. Biogeochemical drivers of the fate of riverine mercury discharged to the global and Arctic oceans. Glob. Biogeochem. Cycles 29, 854–864. https://doi.org/10.1002/2015gb005124.
Zhang, Z., Yao, Z., Hu, L., Anatolii, A., Zou, J., Liu, Y., Wang, K., Yang, G., Chen, Z., Xia, Y., Li, Q., Feng, H., Shi, X., 2023. Distribution characteristics and implications of

mercury in the surface sediments of the East Siberian Arctic Shelf. Mar. Geol. Quat. Geol. 43, 49–60. https://doi.org/10.16562/j.cnki.0256-1492.2022071801.
Zheng, Z., Wei, H., Luo, X., Zhao, W., 2021. Mechanisms of Persistent High primary production during the growing season in the Chukchi Sea. Ecosystems 24, 891–910. https://doi.org/10.1007/s10021-020-00559-8.
Zyrin, N.G., Zvonarev, B.A., Kim, N., 1978. Mercury in the brown forest soils of Dagestan and the northern Osetiya. Moscow Univ. Soil Sci. Bull. 12, 22–26.